Research Article

Received: 8 October 2021 Revised: 12 November 2021 Accepted article published: 17 November 2021 Published online in Wiley Online Library:

(wileyonlinelibrary.com) DOI 10.1002/pi.6330

Evaluation of suitable onium tetrafluoroborates for cationic polymerization of epoxides

Roland Taschner, Robert Liska and Patrick Knaack*

Abstract

Epoxides are frequently used in coatings due to their great adhesion to most materials, high resistance towards chemicals and well-defined material properties. Onium salts such as iodonium and sulfonium salts are one of the most widespread classes of initiators used in light-induced cationic polymerization of such epoxides. We successfully synthesized onium salts based on group 14 to 16 elements in the periodic table. They were then characterized using cyclic voltammetry and UV–visible spectroscopy before determining their reactivity in epoxy-based resins. Using commercial bisphenol-A-based resins, thiopyrylium, bismuthonium and pyrylium salts show good reactivity and epoxy group conversions above 60% in simultaneous thermal analysis. Photochemically interesting new cationic initiators were identified to be oxonium, thiopyrylium and selenonium salts. Additionally, bismuthonium and stibonium salts show great potential towards sensitization with anthracene.

Keywords: cationic polymerization; onium salt; tetrafluoroborate; epoxide

INTRODUCTION

Like most polymerization reactions, cationic polymerization involves a chain growth mechanism. Examples for cationically polymerizable monomers are heterocyclic and unsaturated molecules.[1] Especially, the class of epoxy monomers are capable of achieving material properties unlike radically polymerized resins, such as excellent adhesion and resistance against many chemicals, which are required in inks, films, coatings and adhesives.[2] To start a cationic polymerization, a strong Brønsted or Lewis acid is necessary. These acids provide the proton or carbocation for the initiation step of the reaction. During cationic photopolymerization, most likely a UV photon is absorbed by the cationic initiator, forming an ion, which is capable of starting the polymerization reaction.[2] For simplicity, a cationic initiator activated via photons is described as a photoacid generator.

Ideal photoinitiators for cationic polymerization require chromophores to absorb light of a specific wavelength, in combination with the creation of photoacid in high quantum yields. Thermal stability as well as easy synthesis and low cost are of high importance.[1,3] Photoacid generators such as onium salts are of highest interest, due to efficient photodecomposition, high stability and easy synthesis.[1,4]

Generally, onium salts consist of two ions with clearly separated roles, when it comes to absorption, stability or initiation efficiency properties (Table 1). The cation represents the chromophore and determines all photochemistry-related properties. The anion affects the strength of the generated photoacid, therefore initiation efficiency and all polymer chemistry-related properties.[5]

Iodonium and sulfonium salts

Commonly used in industry are onium salts, containing diaryliodonium and triarylsulfonium as cations. They are the state-of-the-art in onium chemistry, efficient, stable photoacid generators and do not require extensive effort to prepare. The inventors of these compounds were Crivello *et al*. in the 1970s.[4–6]

Irradiation with UV light leads to absorption of photons by the chromophore of the photoacid generator (Fig. 1). This leads to excitation of the molecule towards its singlet state. From there on, the decomposition can happen homolytically or heterolytically.[7] During this cleavage, various products like radical-cations, radicals, cations and aryl halides are formed. If the cleavage occurs homolytically, there is the possibility to convert the decomposition products to the heterolytic ones via electron transfer. In the last step the radical, formed in the homolytic pathway, performs a hydrogen abstraction from the monomer or possibly the solvent to form a Brønsted acid (HX) and a neutral aryl species. In the case of heterolytic cleavage, the phenyl cation performs an electrophilic attack on the monomer or solvent, forming a Brønsted acid (HX) and a neutral aryl species again. The Brønsted acid is in both cases the essential species, capable of initiating the cationic polymerization.[5,8]

* *Correspondence to: P Knaack, Institute of Applied Synthetic Chemistry, TU Wien, Getreidemarkt 9, 1060 Vienna, Austria. E-mail: patrick.knaack@tuwien.ac.at*

Department of Polymer Chemistry and Technology, Institute of Applied Synthetic Chemistry, TU Wien, Vienna, Austria

Table 1. Roles of cation and anion in onium salts[5]

Cation (photochemistry)	Anion (polymer chemistry)
Absorption behavior	Acid strength
Molar absorption coefficient	Nucleophilicity
Quantum yield	Initiation efficiency
Thermal stability	Propagation rate constant

Additionally, it is known that stable onium compounds undergo cleavage, if suitable radical initiators are present in the system.[9] Mentioned radicals are then able to take part in radical-induced cationic polymerization (RICP). For this system to work, abstractable protons, provided by the monomer for example, are necessary.[10]

Onium salts can also be cleaved by sensitization using a suitable molecule with an absorption maximum significantly shifted to longer wavelength.[2] This occurs by electron transfer and, once sensitized, the cation liberates the superacid which can further initiate the cationic polymerization.[1]

In the work reported in this paper we were interested in exploring the performance of several other onium salts in the field of cationic photopolymerization.

Unlike normal trivalent sulfonium salts, the thiopyrylium class is based on a positive charged thiophene ring. The sulfur cation is directly built into the aromatic ring structure, instead of phenyl substituents directly attached to it. This structural change leads to different photochemical behavior in terms of absorption and reactivity.[11]

Group 14 onium salts

In the 1930s Meerwein and van Emster came across the existence of trivalent, positively charged carbon atoms while studying the kinetics of the rearrangement of camphene hydrochloride.[12] While the methylium ion was only an intermediate during the rearrangement, much more stable compounds were introduced later. For instance, tris(4-methoxyphenyl)methylium salts are especially stable due to the distribution of the positive charge over ten carbon atoms (center atom, *para*- and *ortho*-carbon atoms) and the stabilizing effects of three methoxy moieties.

The conversion of germanium center atoms into germanonium cations with bromide as counterion was reported by Kraus and Foster.[13] However not all substituents or counterions are possible for those salts. For instance, the chemically very similar silicon in its trialkyl configuration is not able to form a stable salt with perfluorometallated anions like hexafluoroantimonate at room temperature.[14] However, according to the literature, Edlund *et al.* suggest evidence of organotin cations with weakly coordinating anions only in solution.[15] Due to the high similarity of germanium and tin, neither of the elements could be transformed into the corresponding onium salt.

Group 15 onium salts

The very broad term azonium ions includes a variety of different substance classes. Ammonium, nitrosonium and diazonium ions are common examples just to name a few.[14] Since diazonium compounds are thermally very unstable and release nitrogen gas upon irradiation (either thermal photons or UV photons), their application as cationic photoacid generators is not of interest. Additionally, the free electron pair of diazonium and nitrosonium compounds can act as an inhibiting base, therefore interfering with the propagating, positive charged chain end during cationic polymerization. This leads to ammonium and pyridinium salts as suitable substance class due to their stability and absence of free electron pairs.

Tetravalent phosphor-based compounds were introduced in the early 1960s.[16] Quaternary phosphonium cations are generally produced by alkylation of organophosphines (e.g. triphenylphosphine) with iodides.[17] This reaction route leads to stable phosphonium salts in high yields and which are easy to purify. Due to their high thermal stability, phosphonium salts show low potential as thermal initiators. Investigation of this behavior was performed by Takuma *et al.* and led to the assumption that phosphonium hexafluoroantimonates can act as latent thermal initiators for cationic polymerization of epoxides.[18] When irradiated at their absorption maximum at 268 nm, the phosphonium salts are unable to generate reactive species to induce cationic polymerization.[19]

Similar to tetravalent phosphor compounds, there is the possibility to synthesize antimony-based onium salts. Stibonium hexafluoroantimonates were used to polymerize tetrahydrofuran with triethylsilane as an additive.[20] Therefore the photochemical properties and reactivity of such compounds are very interesting.

Bismuth-based onium salts have the property of being classified as metals, rather than nonmetals and transition metals like phosphonium or stibonium salts. This circumstance makes them an interesting onium class on their own. Previous research

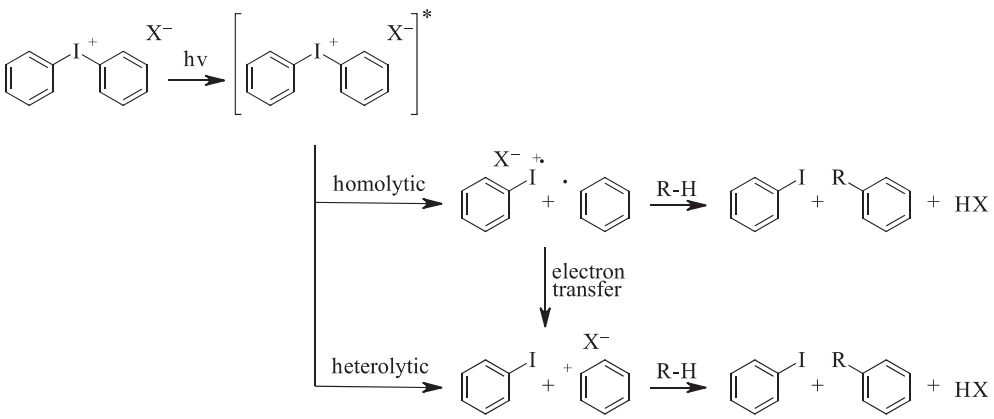

Figure 1. Photochemical decomposition of a diphenyliodonium salt resulting in the liberation of superacid HX.[7]

conducted by Matano *et al.* showed the good photochemical behavior of bismuthonium hexafluoroantimonates in epoxy-based systems as photoacid generators.[21]

Group 16 onium salts

When oxonium compounds are mentioned, usually Meerwein salts[22] are the topic of most interest. Trivalent alkyloxonium salts are generally used in organic chemistry. Tri(m)ethyloxonium tetrafluoroborates for example are highly efficient alkylation agents. However, they suffer from thermal instability and hydrolysis at room temperature. Interestingly, positively charged oxygen atoms bound to phenyl rings experience rather unexpected stability towards temperature and moisture. Triphenyloxonium salts were first investigated by Nesmeyanov *et al.*[23] by the reaction of diphenyl ether with benzenediazonium tetrafluoroborate, while nitrogen gas is released. The rather low yield of the reaction can be improved by forcing an intramolecular nitrogen release instead of an intermolecular one. However, the educt for this improved route is more complicated to obtain.[24] All mentioned oxonium salts to this point have been symmetric ones; however, there is the possibility of generating asymmetric oxonium salts *in situ*, like aryldialkyl- or diarylalky-substituted compounds. The problem of asymmetric oxonium compounds is their instability above −70 °C in solution. Therefore, such asymmetric salts are not able to be isolated due to their immense reactivity towards trans-alkylation.[14,25]

Unlike normal oxonium salts, where the positive charge is carried by a central oxygen atom, pyrylium salts distribute this charge over at least one aromatic ring. The base molecule is a six-membered ring including the oxonium ion. Triphenylpyrylium tetrafluoroborate has shown reactivity towards cationic resins with vinyl ethers as coinitiators.[26]

The preparative aspects of selenonium and other group 16 cations have been compiled in a review by Irgolic.[27] Additionally, Crivello and Lam[28] investigated the photochemical properties of selenonium salts and their potential in acting as acid generators. Therefore, this class of onium compounds was included in the studies.

In contrast to group 15 non-metals, for example sulfonium and selenonium salts, the telluronium compounds are part of the transition metals located in the fifth period of the periodic table of elements. Therefore, the photochemical properties are expected to change due to the more metal-like behavior of telluronium salts. This makes them an interesting component of the selected compounds for further testing. Synthesis of tellurium-based onium salts is a well understood process and is possible in high yields.[27]

In this paper, the industry-leading onium salts diaryliodonium and triarylsulfonium are challenged. A variety of different central atoms for onium salts are investigated on the path towards new acid generators suitable for initiating cationic polymerization. The onium tetrafluoroborates are compared in terms of photochemical behavior, electrochemical potential, reactivity and initiation versatility in an epoxy-based system.

EXPERIMENTAL

Materials and methods

Phenylboronic acid, 95%, CAS: 98-80-6, Sigma Aldrich; boron trifluoride dibutyl etherate (BF_3-Et_2O), quality level 100, CAS: 593-04-4, Sigma Aldrich; (diacetoxyiodo)benzene, 98%, CAS: 3240-34-4, Sigma Aldrich; diphenyliodonium chloride, 98%, CAS: 1483-72-3, Sigma Aldrich; sodium hexafluoroantimonate, technical grade, CAS: 16925-25-0, Sigma Aldrich; triphenylsulfonium chloride, 94%, CAS: 4270-70-6, Alfa Aesar; sodium tetrafluoroborate, 98%, CAS: 13755-29-8, Sigma Aldrich; 2,4,6-triphenylpyrylium tetrafluoroborate (3PP-O-BF_4), 97%, CAS: 448-61-3, ChemPUR; tetrafluoroboric acid, 50% in water, CAS: 1687211-0, Alfa Aesar; triphenylantimony dichloride, 99%, CAS: 603-36-1, Sigma Aldrich; phenylmagnesium bromide (3 mol L^{-1} in diethyl ether), CAS: 100-58-3, Sigma Aldrich; hydrobromic acid (40% in water), CAS: 10035-10-6, Alfa Aesar; tetraphenylphosphonium bromide (4P-P-Br); 98%, CAS: 2751-90-8, TCI; triphenylbismuth, 99%, CAS: 603-33-8, ABCR; sulfonyl chloride, 97%, CAS: 7791-25-5, Sigma Aldrich; potassium fluoride, 99%, CAS: 7789-23-3, Sigma Aldrich; phenylboronic acid, 98%, CAS: 98-80-6, ChemPUR; aniline, 98%, CAS: 62-53-3, TCI; sodium nitrite, 98.5%, CAS: 7632-00-0, TCI; diphenyl ether, 99%, CAS: 101-84-8, ABCR; diphenyl selenide, 98%, 1132-39-4, ABCR; aluminium chloride, 99.99%, anhydrous, CAS: 7446-70-0, ABCR; benzene, 99.8, CAS: 71-43-2, Sigma Aldrich; tellurium tetrachloride, 99.9%, CAS: 10026-07-0, ABCR; 1-butyl-4-methylpyridinium tetrafluoroborate (BuMeP-N-BF_4), 97%, CAS: 343952-33-0, Sigma Aldrich; 1,1,2,2-tetraphenyl-1,2-ethanediol (TPED), 95%, CAS: 464-72-2, TCI; bisphenol A diglycidyl ether (BADGE), Araldite MY 790-1, CAS: 1675-54-3, Huntsman; propylene carbonate (PC), 97.7% anhydrous, CAS: 108-32-7, Sigma Aldrich; anthracene, 97%, CAS: 120-12-7, TCI; tetraethylammonium tetrafluoroborate, 99%, CAS: 429-06-1, Sigma Aldrich; acetonitrile, 99.98% HPLC grade, CAS: 75-05-8, VWR. All chemicals and solvents were used as received if not mentioned otherwise in the synthesis section. NMR spectra were recorded with a Bruker Avance at 400 MHz for ^{1}H, 100 MHz for ^{13}C, 162 MHz for ^{31}P and 376 MHz for ^{19}F. The signals were always referenced to the NMR solvent used with a deuterium grade of at least 99.5%.

Synthesis

Diphenyliodonium tetrafluoroborate (2P-I-BF_4)

To synthesize 2P-I-BF_4, a reaction route according to Korwar *et al.*[29] was adopted (Fig. 2(a)). At first, 1 eq. (0.359 g, 3 mmol) of phenylboronic acid and 15 mL of dichloromethane were weighed into a 50 mL flask, which was purged with argon gas and cooled with an ice bath to 0 °C. The flask was equipped with a septum and an argon balloon to protect the reaction mixture from the atmosphere. To this clear solution 1.1 eq. (0.4 mL, 3.3 mmol) of boron trifluoride etherate was added dropwise over 5 min. The solution was stirred for 15 min. After this step, 1 eq. (1.056 g, 3 mmol) of diacetoxyiodobenzene dissolved in 10 mL of dichloromethane was added and the mixture stirred for 1.5 h at 0 °C. In the last step, 3.5 mL of saturated sodium tetrafluoroborate solution in water was added and the mixture stirred for 30 min. Then 50 mL of deionized water was added to the reaction mixture, the phases separated and the organic layer was washed twice with 50 mL of water afterwards. The combined aqueous layers were extracted once with 25 mL of dichloromethane. The combined organic layers were dried with sodium sulfate and the solvent was removed using a rotary evaporator. No product was obtained. The aqueous layer was evaporated to a volume of approximately 4 mL and extracted with 25 mL of dichloromethane. The organic layer was dried and a white precipitate was obtained, which was washed with a mixture of 3:1 petroleum ether and dichloromethane. The white powder was washed with 3 × 20 mL of petroleum ether and then dried using a rotary evaporator, yielding 0.291 g (27% of theory) of 2P-I-BF_4.

Polymer International published by John Wiley & Sons Ltd on behalf of Society of Industrial Chemistry.

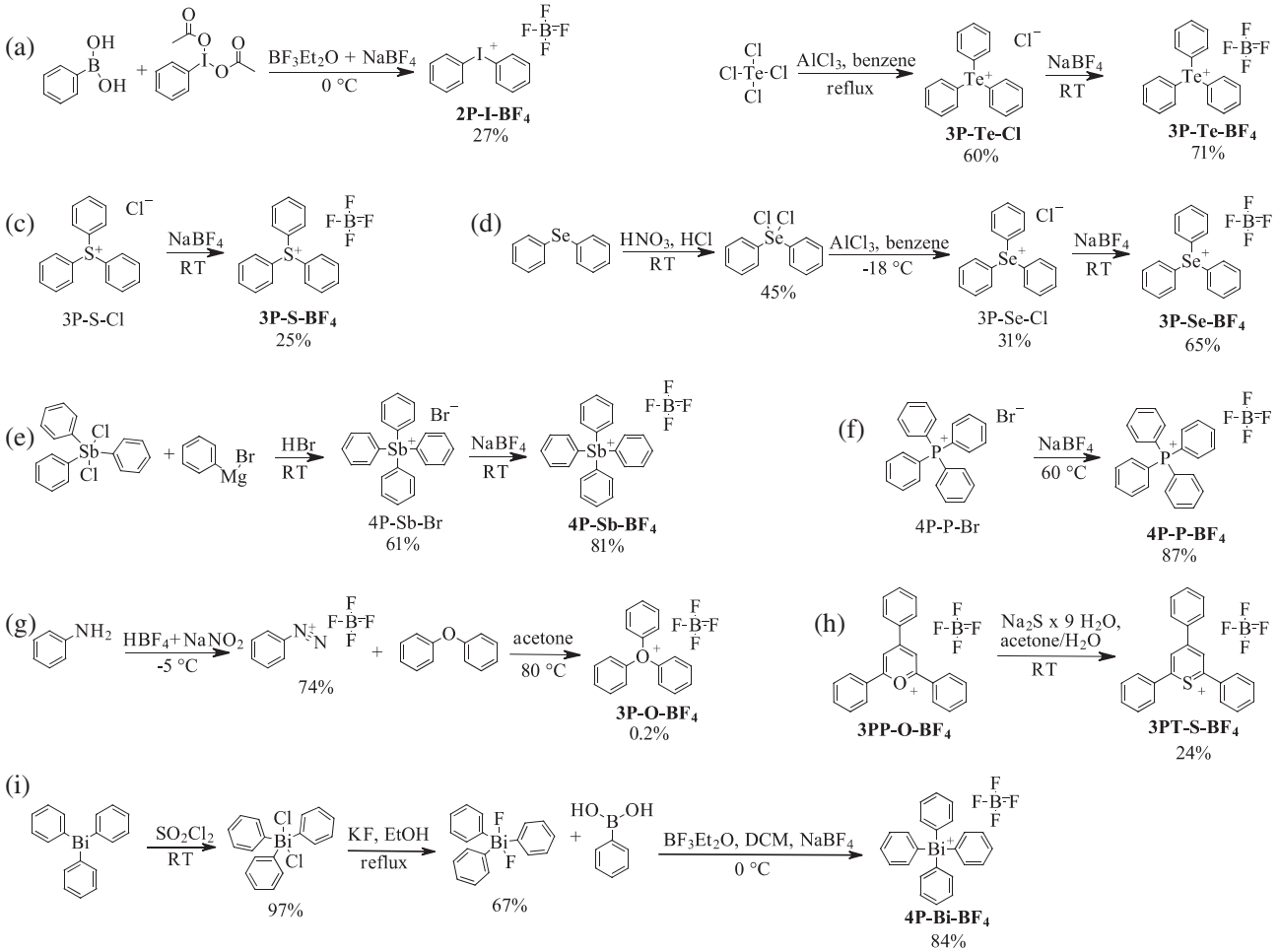

Figure 2. Synthesis pathways to tetrafluoroborates: (a) diphenyliodonium; (b) triphenyltelluronium; (c) triphenylsulfonium; (d) triphenylselenonium; (e) tetraphenylstibonium; (f) tetraphenylphosphonium; (g) triphenyloxonium; (h) 2,4,6-triphenylthiopyrylium; (i) triphenylbismuthonium.

Melting point: 137.6–139.7 °C (lit. 135–136 °C)[30]; ^{1}H NMR (400 MHz, $CDCl_3$): 8.02 (d, 4H, 4× C–C*H*), 7.64 (t, 2H, 2× C–CH–CH–C*H*), 7.48 (t, 4H, C–C*H*–CH), 7.26 (s, $CDCl_3$); ^{13}C NMR (100 MHz, $CDCl_3$): 135.5 (s, 4× C–CH), 133.1 (s, 2× P–C–CH–CH–*C*H), 132.8 (s, 4× C–CH–*C*H), 112.3 (s, 2× *C*), 77.2 (t, $CDCl_3$); ^{19}F NMR (376 MHz, $CDCl_3$): −150.18 (s, BF_4), −150.24 (s, BF_4).

Triphenylsulfonium tetrafluoroborate (3P-S-BF_4)

To synthesize 3P-S-BF_4, an ion exchange similar to that reported by Li *et al.*[31] was performed (Fig. 2(c)). At first, 1 eq. (0.508 g, 1.7 mmol) of triphenylsulfonium chloride and 10 mL of deionized water were weighed into a 50 mL flask. To this clear solution 1.1 eq. (0.206 g, 1.9 mmol) of sodium tetrafluoroborate, dissolved in 2 mL of deionized water, was added. A white precipitate was formed immediately. The mixture was stirred for 45 min. Next the dispersion was filtered using a glass frit and washed with 2 × 25 mL of deionized water, followed by 1 × 25 mL of diethyl ether. The white solid was then dried using a rotary evaporator, yielding 0.148 g (25% of theory) of 3P-S-BF_4.

Melting point: 191.3–193.4 °C (lit. 186–187 °C)[32]; ^{1}H NMR (600 MHz, $CDCl_3$): 7.78–7.75 (m, 3H, 3× S–C–CH–CH–CH–C*H*), 7.73–7.69 (m, 12H, 6× S–C–CH–C*H* and 6× S–C–C*H*), 7.26 (s, $CDCl_3$); ^{13}C NMR (150 MHz, $CDCl_3$): 134.9 (s, 3× S–C–CH–CH–*C*H), 131.9 (s, 6× S–C–CH–*C*H), 131.4 (s, 6× S–C–*C*H), 124.6 (d, 3× S–*C*), 77.2 (t, $CDCl_3$); ^{19}F NMR (376 MHz, $CDCl_3$): −150.27 (s, BF_4), −150.32 (s, BF_4).

2,4,6-Triphenylthiopyrylium tetrafluoroborate (3PT-S-BF_4)

To synthesize 3PT-S-BF_4, a reaction route according to Michaudel *et al.*[33] was adopted (Fig. 2(h)). At first, 1 eq. (1.128 g, 2.8 mmol) of 3PP-O-BF_4 was weighed into a flask and dissolved in 15 mL of acetone by gently applying heat. In a separate container, 4 eq. (3.70 g, 11.2 mmol) of sodium sulfide nonahydrate was dissolved in 10 mL of deionized water. The clear solution of sodium sulfide was added to a stirred clear solution of 2,4,6-triphenylpyrylium tetrafluoroborate. During the addition, the solution turned from yellow to red and was stirred for 1 h. Afterwards the red solution was added to 50 mL of stirred tetrafluoroboric acid (50 wt% in water) in an Erlenmeyer flask. A yellow precipitate started to form immediately and after 1 h of stirring, the yellow solid was filtered via a glass frit and washed with 20 mL of diethyl ether. The product (around 0.7 g) was then dried in vacuum and afterwards recrystallized from 3 mL of acetonitrile. Due to insoluble parts, the dispersion was hot-filtered and the filter paper purged with another 3 mL of acetonitrile to contain as much product as possible. By applying heat to the flask, the volume of acetonitrile was reduced to around 3 mL. The flask was allowed to cool to room temperature, before being transferred to a colder environment at 2 °C. Yellow needles formed over the course of a few hours. The crystals

were filtered via a glass frit and dried in vacuum to finally yield 0.302 g (24% of theory) of 2,4,6-triphenylthiopyrylium tetrafluoroborate as yellow crystals.

Melting point: 193.6–197.8 °C (lit. 195–199 °C)[34]; ^{1}H NMR (600 MHz, CD_3CN): 9.01 (s, 2H, 2× S–C–*CH*), 8.21–8.17 (m, 2H, 2× S–C–CH–C–C–*CH*), 8.12–8.09 (m, 4H, 4× S–C–C–*CH*), 7.86–7.73 (m, 9H, 6× C–C–CH–*CH*; 3× C–C–CH–CH–*CH*), 7.26 (s, $CDCl_3$); ^{13}C NMR (150 MHz, CD_3CN): 171.0 (s, 2× S–*C*), 163.5 (s, S–C–CH–*C*), 138.0 (s, S–C–CH–C–*C*), 135.5 (s, 2× S–C–*C*), 135.3 (s, 2× S–C–*C*H), 135.0 (s, S–C–CH–C–C–CH–CH–*C*H), 132.6 (s, 2× S–C–C–CH–CH–*C*H), 131.7 (s, 4× S–C–C–*C*H), 131.4 (s, 2× S–C–CH–C–C–*C*H), 131.1 (s, 2× S–C–CH–C–C–CH–*C*H), 130.2 (s, 4× S–C–C–CH–*C*H), 118.7 (s, CD_3CN), 1.4 (sep, CD_3CN); ^{19}F NMR (564 MHz, CD_3CN): −151.79 (s, B*F*$_4$), −151.84 (s, B*F*$_4$).

Tetraphenylphosphonium tetrafluoroborate (4P-P-BF$_4$)

To synthesize 4P-P-BF$_4$, an ion exchange similar to that reported by Li *et al.*[31] was performed (Fig. 2(f)). At first, 1 eq. (1.048 g, 2.5 mmol) of 4P-P-Br and 20 mL of a mixture of methanol and deionized water (1:3) were weighed into a 50 mL flask, equipped with a condenser. The dispersion was magnetically stirred and heated to 60 °C, until the educt was completely dissolved. To this clear solution 1.1 eq. (0.304 g, 2.8 mmol) of sodium tetrafluoroborate, dissolved in 1 mL of deionized water, was added. A white precipitate was formed immediately. The heating bath was removed and the mixture was allowed to cool to room temperature, where it was further stirred for 2 h. Next the dispersion was filtered using a glass frit and washed with 2 × 25 mL of a mixture of methanol and deionized water (1:3), followed by 25 mL of diethyl ether. The solid, white powder was then dried using a rotary evaporator, yielding 0.925 g (87% of theory) of 4P-P-BF$_4$.

Melting point: 351.1–353.8 °C (lit. 350.5 °C)[32]; ^{1}H NMR (400 MHz, $CDCl_3$): 7.91–7.86 (m, 4H, 4× P–C–CH–CH–C*H*), 7.80–7.75 (m, 8H, 8× P–C–CH–C*H*), 7.67–7.62 (m, 8H, 8× P–C–*CH*), 7.26 (s, $CDCl_3$); ^{13}C NMR (100 MHz, $CDCl_3$): 135.9 (d, 4× P–C–CH–CH–*C*H), 134.7 (d, 8× P–C–CH–*C*H), 130.9 (d, 8× P–C–*C*H), 117.4 (d, 4× P–*C*), 77.2 (t, $CDCl_3$); ^{31}P NMR (162 MHz, $CDCl_3$): 23.1 (s, 1P); ^{19}F NMR (376 MHz, $CDCl_3$): −150.71 (s, B*F*$_4$), −150.75 (s, B*F*$_4$).

Tetraphenylstibonium bromide (4P-Sb-Br)

To synthesize 4P-Sb-Br, a reaction route according to Ma *et al.*[35] was adopted (Fig. 2(e)). At first, 1 eq. (1.950 g, 4.6 mmol) of triphenylantimony dichloride was weighed into a 50 mL two-necked flask in a glove box to avoid hydrolysis of the precursor. Afterwards the antimony educt was dissolved in 12.3 mL of dry diethyl ether and 6.1 mL of dry toluene. The obtained solution was kept under argon for later use. In the meantime, 3 eq. (4.6 mL, 13.8 mmol) of phenylmagnesium bromide (3 mol L^{-1} in diethyl ether) and 24.6 mL of dry diethyl ether were transferred into a 100 mL two necked-flask under Schlenk line conditions and stirred magnetically. Then the triphenylantimony dichloride solution was added dropwise over 10 min to the phenylmagnesium bromide solution while stirring vigorously. By the use of a water bath, room temperature was maintained over the course of the reaction. After around 5 min the clear solution started to form some precipitate. The resulting dispersion was stirred for 8 days. Then 1.7 g of ice and 2.2 mL of hydrobromic acid (40% in water) were added and the mixture stirred overnight. The yellowish precipitate was filtered off using a glass frit and washed with 30 mL of a 1:2 mixture of toluene and diethyl ether. The solid powder was recrystallized from 10 mL of a 3:2 mixture of water and ethanol. After filtration, washing with diethyl ether and drying in vacuum, 1.662 g (61% of theory) of 4P-Sb-Br as white crystals was obtained.

Melting point: 209.1–212.9 °C (lit. 210–215 °C)[35]; ^{1}H NMR (400 MHz, $CDCl_3$): 7.81–7.78 (m, 8H, 8× C–*CH*), 7.56–7.46 (m, 12H, 8× C–CH–*CH*, 4× C–CH–CH–*CH*), 7.26 (s, $CDCl_3$); ^{13}C NMR (100 MHz, $CDCl_3$): 135.5 (s, 8× C–*C*H), 131.5 (s, 4× C–CH–CH–*C*H), 129.8 (s, 8× C–CH–*C*H), 127.1 (s, 4× Sb–*C*), 77.2 (t, $CDCl_3$).

Tetraphenylstibonium tetrafluoroborate (4P-Sb-BF$_4$)

4P-Sb-Br was used in a procedure similar to that reported by Li *et al.*,[31] for an ion exchange reaction (Fig. 2(e)). To prepare 4P-Sb-BF$_4$, at first 1 eq. (0.589 g, 1 mmol) of 4P-Sb-Br was dissolved in 16 mL of a 5:3 mixture of deionized water and methanol by gently applying heat to result in a clear solution. In the meantime, 3 eq. (0.346 g, 3 mmol) of sodium tetrafluoroborate was dissolved in 4 mL of a 5:3 mixture of deionized water and methanol. A clear solution was obtained after heating the mixture gently. After both solutions were allowed to cool to room temperature, their transparency was checked before moving on to the next step. The clear sodium tetrafluoroborate solution was added dropwise into the clear tetraphenylstibonium bromide solution. A white precipitate started to form immediately and after 15 min of reaction time the reaction mixture was transferred into a tube which was centrifuged at 35 °C. The elevated temperature was used to keep possibly remaining educt (4P-Sb-Br) for sure in solution. The fluid phase was discarded and the solid mixed with 18 mL of a 5:4 mixture of deionized water and methanol to remove excess sodium tetrafluoroborate. The mixture was centrifuged again at 35 °C and the washing fluid was discarded. After drying in vacuum, 4P-Sb-BF$_4$ yielded 0.483 g (81% of theory) as a white powder.

Melting point: 274.7–277.0 °C (lit 265 °C)[32]; ^{1}H NMR (400 MHz, DMSO): 7.83–7.75 (m, 8H, 8× C–*CH*), 7.74–7.63 (m, 12H, 8× C–CH–*CH*, 4× C–CH–CH–*CH*), 2.5 (s, DMSO); ^{13}C NMR (100 MHz, DMSO): 135.2 (s, 8× C–*C*H), 132.4 (s, 4× C–CH–CH–*C*H), 130.4 (s, 8× C–CH–*C*H), 128.8 (s, 4× Sb–*C*), 39.5 (sep, DMSO); ^{19}F NMR (376 MHz, DMSO): −148.27 (s, B*F*$_4$), −148.32 (s, B*F*$_4$).

Triphenylbismuth dichloride

To synthesize triphenylbismuth dichloride, a reaction route according to Solyntjes *et al.*[36] was adopted (Fig. 2(i)). First, 1 eq. of triphenylbismuth (2.815 g, 6.4 mmol) was dissolved in 36 mL of dry dichloromethane. The mixture was magnetically stirred in a 50 mL round-bottom flask equipped with a septum and was set under argon back pressure. Then 1.4 eq. of sulfonyl chloride (0.72 mL, 9 mmol) was added dropwise over 5 min. During the addition, SO_2 gas was formed. The mixture was stirred for 1 h. The solvent and residual sulfonyl chloride were evaporated at 50 °C and the remaining whitish solids were used in the next step without further purification. The reaction yielded 3.161 g (97% of theory) of triphenylbismuth dichloride.

Melting point: 136.8–140.5 °C (lit. 149–150 °C)[37]; ^{1}H NMR (400 MHz, DMSO): 7.53 (d, 6H, 6× C–C*H*), 6.93 (t, 6H, 6× C–CH–*CH*), 6.78 (t, 3H, 3× C–CH–CH–*CH*), 2.50 (s, DMSO); ^{13}C NMR (100 MHz, DMSO): 156.2 (s, 4× Bi–*C*), 129.7 (s, 8× C–*C*H), 127.7 (s, 8× C–CH–*C*H), 127.2 (s, 4× C–CH–CH–*C*H), 39.51 (sep, DMSO).

Triphenylbismuth difluoride

To synthesize triphenylbismuth difluoride, a reaction route according to Challenger and Wilkinson[38] was adopted (Fig. 2(i)). First, 1 eq. of triphenylbismuth dichloride (7.233 g, 14.2 mmol) and 3 eq. of potassium fluoride (2.466 g, 42.5 mmol) were weighed into a 250 mL one-necked round-bottom flask equipped

Polymer International published by John Wiley & Sons Ltd on behalf of Society of Industrial Chemistry.

with a condenser. The starting materials were dispersed in 100 mL of ethanol and 1 mL of deionized water. The mixture was refluxed for 20 h. The solids were filtered off with a glass frit and discarded. The filtrate was evaporated to dryness *in vacuo* to give a yellowish-beige solid, which was washed with 3 × 20 mL of hot deionized water. Purification was carried out by washing the product with 20 mL of cold (−20 °C) diethyl ether. The beige solid was dried in vacuum and yielded 4.505 g (67% of theory) of triphenylbismuth difluoride.

Melting point: 155.3–162.1 °C (lit. 159–161 °C)[39]; ^{1}H NMR (400 MHz, DMSO): 8.10 (d, 6H, 6× C–C*H*), 7.74 (t, 6H, 6× C–CH–C*H*), 7.58 (t, 3H, 3× C–CH–CH–C*H*), 2.50 (s, DMSO); ^{13}C NMR (100 MHz, DMSO): 144.0 (s, 4× Bi–*C*), 135.7 (s, 8× C–*C*H), 131.6 (s, 8× C–CH–*C*H), 131.4 (s, 4× C–CH–CH–*C*H), 39.51 (sep, DMSO); ^{19}F NMR (376 MHz, DMSO): −153.4 (s, 2× Bi–*F*).

Tetraphenylbismuthonium tetrafluoroborate (4P-Bi-BF_4)

To synthesize 4P-Bi-BF_4, a reaction route according to Matano *et al.*[40] was carried out (Fig. 2(i)). The starting materials were weighed out in a glove box in order to avoid hydrolysis of the precursor. At first, 1 eq. of triphenylbismuth difluoride (0.478 g, 1 mmol) and 1 eq. of phenylboronic acid (0.122 g, 1 mmol) were suspended in 10 mL of dry dichloromethane. The suspension was set under an argon atmosphere, cooled to 0 °C and magnetically stirred. Then 1 eq. of BF_3 diethyl etherate (0.125 mL, 1 mmol) was slowly added dropwise to the suspension, which resulted in a clear solution. After the addition, the ice bath was removed and the reaction solution was further stirred at room temperature. During the course of the reaction, intermediately some white precipitate started to form, which dissolved after some time again. After a total of 2 h of reaction time, a solution of 9.1 eq. of $NaBF_4$ (1.001 g, 9.1 mmol) in 40 mL of deionized water was added dropwise to the reaction solution. The mixture was then stirred vigorously for 0.5 h. The layers were then separated and the aqueous layer extracted twice with 10 mL of dichloromethane. The combined organic layers were dried with Na_2SO_4, filtered (filter washed with additional 5 mL of dichloromethane) and the solvent was removed using a rotary evaporator. The crude product resulted in 0.588 g of white crystals which were purified by recrystallization (31 mL with a ratio of 1:1.5 of diethyl ether to ethanol). The solution was allowed to cool to room temperature and then stored at 2 °C. The crystals were filtered via a glass frit (washed with additional 2 mL of ethanol) and dried in vacuum to finally yield 0.460 g of tetraphenylbismuthonium tetrafluoroborate as white crystals in the first fraction. Additionally, the residual solution was concentrated in vacuum to yield a further 0.049 g of 4P-Bi-BF_4. Hence a total yield of 0.509 g (84% of theory) was obtained as pure tetraphenylbismuthonium tetrafluoroborate.

Melting point: 246.0–248.0 °C (lit. 243–244 °C)[40]; ^{1}H NMR (400 MHz, $CDCl_3$): 7.80 (d, 8H, 8× C–C*H*), 7.68 (t, 8H, 8× C–CH–C*H*), 7.62 (t, 4H, 4× C–CH–CH–C*H*), 7.26 (s, $CDCl_3$); ^{13}C NMR (100 MHz, $CDCl_3$): 137.8 (s, 4× Bi–*C*), 136.1 (s, 8× C–CH), 132.7 (s, 8× C–CH–*C*H), 132.6 (s, 4× C–CH–CH–*C*H), 77.23 (t, $CDCl_3$); ^{19}F NMR (376 MHz, $CDCl_3$): −149.65 (s, B*F_4*), −149.70 (s, B*F_4*).

Benzenediazonium tetrafluoroborate

Benzenediazonium tetrafluoroborate was synthesized according to Flood,[41] with the exception of using directly tetrafluoroboric acid instead of hydrochloric acid in the first step and therefore skipping the ion exchange afterwards (Fig. 2(g)). At first 2.1 eq. (26 mL, 105 mmol) of tetrafluoroboric acid (50 wt% in water) and additional 12 mL of deionized water were cooled to −5 to −10 °C in a three-necked flask with a sodium chloride ice bath. The fluid was mechanically stirred due to the formation of a white, thick mixture after the addition of 1 eq. (4.85 mL, 50 mmol) of distilled aniline. After the mixture was stirred for 15 min, 1.05 eq. (3.622 g, 52.5 mmol) of sodium nitrite was dissolved in 10 mL of distilled water, cooled to −5 °C and added dropwise over 1 h. During this step the mixture was not allowed to reach a temperature above 0 °C. The slightly yellow-orange magma was then stirred for 1 h at −5 °C and afterwards the precipitated filtered using a glass frit. The solids were washed with 50 mL of iced deionized water, followed by 50 mL of cold methanol, 50 mL of cold diethyl ether and finally 50 mL of cold hexanes. After the washing procedure the solid white powder was pre-dried in a glass frit by sucking air through the funnel for around 5 min. The benzenediazonium tetrafluoroborate yielded 7.1 g (74% of theory) as a white powder. A quick approach to verify the presence of diazonium salts is the formation of nitrogen gas bubbles in around 10 to 20 min if exposed to sunlight in a DMSO solution in a small-diameter tube sitting at an angle. The product was used directly for the next reaction step after the 5 min drying procedure in the glass frit even though it was slightly wet due to the hexanes which were not removed completely during the process. For the NMR analysis, a small part of the diazonium salt was dried overnight in a desiccator while applying a slight vacuum (800 mbar).

^{1}H NMR (400 MHz, acetone-d_6): 8.82 (d, 2H, 2× C–C*H*), 8.37 (t, 1H, C–CH–CH–C*H*), 8.07 (t, 2H, 2× C–CH–C*H*), 2.05 (q, acetone); ^{13}C NMR (100 MHz, acetone-d_6): 206.8 (s, acetone), 155.3 (s, *C*), 129.9 (s, 2× C–CH–*C*H), 120.6 (s, C–CH–CH–*C*H), 115.3 (s, 2× C–*C*H), 29.9 (sept, acetone); ^{19}F NMR (376 MHz, acetone-d_6): −150.79 (s, B*F_4*), −150.84 (s, B*F_4*).

Triphenyloxonium tetrafluoroborate (3P-O-BF_4)

To synthesize 3P-O-BF_4, a reaction similar to that of Nesmeianov *et al.*[23] was carried out (Fig. 2(g)). An excess of diphenyl ether was reacted with a benzenediazonium tetrafluoroborate solution. An amount of 1 eq. of benzyldiazonium tetrafluoroborate (7 g, 36.5 mmol) was dissolved in 300 mL of cold distilled acetone and kept in a beaker in a sodium chloride ice bath at −5 °C. It was reacted dropwise over 1 h with 16 eq. of diphenyl ether (99.9 g, 584 mmol) which was preheated to 80 °C in a flask under argon atmosphere. During the addition of the diazonium salt the solution turned from colorless to yellow to red. After refluxing for 0.5 h, the mixture was cooled to room temperature and stirred overnight. The acetone was evaporated using a rotary evaporator. Afterwards 20 mL of a 1:1 mixture of acetone and deionized water were added and the layers separated. The extraction was performed again with another 20 mL of the acetone–water mixture. The acetone–water layers were combined and extracted with 40 mL of diethyl ether and the layers were separated. The evaporation of the acetone–water layer should result in the precipitation of the oxonium salt after the acetone was removed due to the insolubility of oxonium salts in water. This did not happen during the acetone evaporation. Therefore, the residual aqueous layer was combined with the residues of the evaporated diethyl ether layer to perform a different workup. This time 80 mL of hexanes was added and a white precipitate started to form at the phase boundary. The white solids were filtered using a glass frit and washed with 20 mL of deionized water. Then the solid powder was dissolved in 40 mL of distilled acetone and transferred into a flask, where the solvent was evaporated using a rotary evaporator. The whitish crystals were dried using a high-vacuum pump for 10 min. After the workup of fraction 1, additional white

solids precipitated out of the aqueous layer after around 15 min (where the 80 mL of hexanes were added previously). The solids were filtered, washed with water and transferred with acetone into a flask where the solvents were evaporated and the crystals dried in high vacuum, resulting in fraction 2. For purification the two fractions were combined and dissolved in 2 mL of distilled acetone in a centrifuge tube just to be precipitated by the addition of 3 mL of hexanes. After 5 min of centrifuging at 10 °C (5000 rpm) the solvent was decanted off and kept in another centrifuge tube. This precipitation was executed again to improve the purity of the triphenyloxonium tetrafluoroborate even more before drying the white crystals in vacuum. Therefore fraction 1 was obtained as white crystals (21 mg, m_p = 241.9 °C decomp.). The combined decanted solvents (acetone–hexanes) were stored at 2 °C and led to additional precipitate after 30 min. The dispersion was centrifuged and the solvent decanted off into another centrifuge tube. Fraction 2 was dried in vacuum and yielded white crystals (5 mg, m_p = 240.7 °C decomp.). Afterwards the acetone–hexanes were stored at −18 °C overnight. Again, additional crystals started to form and were centrifuged. Fraction 3 was dried in vacuum and yielded white crystals (4 mg, m_p = 236.4 °C decomp.). In combination a total yield of 30 mg (0.2% of theory) of triphenyloxonium tetrafluoroborate was obtained as white crystals.

Melting point: 241.9 °C (decomposition) (lit. 226 °C decomp.)[23]; ^{1}H NMR (600 MHz, acetone-d_6): 8.13 (d, 6H, 6× C–C*H*), 7.81 (t, 6H, 6× C–CH–C*H*), 7.75 (d, 3H, 3× C–CH–CH–C*H*), 2.05 (q, acetone); ^{13}C NMR (150 MHz, acetone-d_6): 206.8 (s, acetone), 161.6 (s, 3× *C*), 133.2 (s, 6× C–CH–*C*H), 132.4 (s, 3× C–CH–CH–*C*H), 121.5 (s, 6× C–*C*H), 29.9 (sept, acetone); ^{19}F NMR (565 MHz, acetone-d_6): −151.26 (s, B*F*$_4$), −151.31 (s, B*F*$_4$).

Dichlorodiphenyl selenide

The synthesis was carried out according to the work of Crivello and Lam[28] (Fig. 2(d)) At first, 1 eq. (2.543 g, 11 mmol) of diphenyl selenide was added into a 25 mL round-bottom flask, which was cooled by a bath of cold water. Then 11 eq. (5 mL, 121 mmol) of concentrated nitric acid was added, resulting in exothermic gas formation. After magnetically stirring for 30 min, 9 eq. (3 mL, 99 mmol) of concentrated hydrochloric acid was added, leading to an immediate formation of a yellow precipitate. The dispersion was stirred for 5 min and filtered using a glass frit. This resulted in a solid, yellow product, which was further washed with 70 mL of deionized water. Using a rotary evaporator, the product was dried, yielding 1.844 g of dichlorodiphenyl selenide as yellow powder. Due to a broad melting interval, the purity of the product was improved via recrystallization from about 14 mL of dry benzene. The crystals were washed with 25 mL of cold methanol, dried using a rotary evaporator and yielded 1.490 g (45% of theory) as yellowish crystals.

Melting point: 180.2–183.6 °C (lit. 181–183 °C)[42]; ^{1}H NMR (400 MHz, $CDCl_3$): 8.06–7.99 (m, 4H, 4× Se–C–C*H*), 7.60–7.51 (m, 6H, 4× Se–C–CH–C*H*, 2× Se–C–CH–CH–C*H*), 7.26 (s, $CDCl_3$); ^{13}C NMR (100 MHz, $CDCl_3$): 142.7 (s, 2× Se–*C*), 132.0 (s, 2× Se–C–CH–CH–CH), 131.5 (s, 4× Se–C–*C*H), 130.0 (s, 4× Se–C–CH–*C*H), 77.2 (t, $CDCl_3$).

Triphenylselenonium chloride (3P-Se-BF$_4$)

In the second step (Fig. 2(d)), 4.5 eq. (2.957 g, 22.1 mmol) of aluminium chloride was weighed into a 50 mL three-necked round-bottom flask and dispersed using 22.5 eq. (10 mL, 110 mmol) of dry benzene. The flask was equipped with a condenser, which was attached to a drying tube filled with calcium chloride and was purged with argon once. The mixture was magnetically stirred and cooled to −18 °C via a sodium chloride ice bath. Over 10 min, 1 eq. (1.490 g, 4.9 mmol) of dichlorodiphenyl selenide was added to the dispersion, resulting in a red-brown solution. To quantitatively transfer the remaining selenide into the flask, another 22.5 eq. (10 mL, 110 mmol) of dry benzene was used. After the addition of the selenide was complete, the cooling bath was removed and the mixture was allowed to heat up to room temperature, continuously stirring for 4 h. Now 40 mL of deionized water was added cautiously (exothermic reaction) and two phases formed in the flask. The upper benzene layer was discarded and the aqueous layer was extracted three times with 40 mL of dichloromethane. The combined organic layers were evaporated using a rotary evaporator. The residue was a yellowish oil, which was washed with 75 mL of diethyl ether dried using a rotary evaporator. After the drying procedure, 3P-Se-Cl yielded 0.529 g (31% of theory) as a yellowish powder.

Melting point: 217.6–221.6 °C; ^{1}H NMR (400 MHz, $CDCl_3$): 7.77–7.73 (m, 6H, 6× Se–C–C*H*), 7.66–7.54 (m, 9H, 6× Se–C–CH–C*H*, 3× Se–C–CH–CH–C*H*), 7.26 (s, $CDCl_3$); ^{13}C NMR (100 MHz, $CDCl_3$): 133.1 (s, 3× Se–C–CH–CH–*C*H), 131.8 (s, 6× Se–C–*C*H), 131.3 (s, 6× Se–C–CH–*C*H), 128.7 (s, 3× Se*C*), 77.2 (t, $CDCl_3$).

Triphenylselenonium tetrafluoroborate (3P-Se-BF$_4$)

In the last step (Fig. 2(d)), 1 eq. (0.529 g, 1.53 mmol) of 3P-Se-Cl was weighed into a 50 mL round-bottom flask and diluted with 6.2 mL of deionized water. Then 1 eq. (0.170 g, 1.53 mmol) of a sodium tetrafluoroborate solution in 1.7 mL of deionized water was added dropwise, under vigorous magnetic stirring, into the flask. A yellowish precipitate formed immediately and the dispersion was stirred for 5 min, before filtering the solid product using a glass frit. The product was washed twice with 10 mL of deionized water and once with 10 mL of cold diethyl ether. After removing the solvent residues using a rotary evaporator, the product 3P-Se-BF$_4$ was afforded as a yellowish powder, yielding 0.397 g (65% of theory).

Melting point: 184.3–186.4 °C (lit. 183–185 °C)[28]; ^{1}H NMR (400 MHz, $CDCl_3$): 7.74–7.69 (m, 3H, 3× Se–C–CH–CH–C*H*), 7.67–7.59 (m, 12H, 6× Se–C–C*H*, 6× Se–C–CH–C*H*), 7.26 (s, $CDCl_3$); ^{13}C NMR (100 MHz, $CDCl_3$): 133.9 (s, 3× Se–C–CH–CH–*C*H), 131.8 (s, 6× Se–C–*C*H), 131.4 (s, 6× Se–C–CH–*C*H), 126.6 (s, 3× Se–*C*), 77.2 (t, $CDCl_3$); ^{19}F NMR (376 MHz, acetone-d_6): −147.41 (s, B*F*$_4$), −147.46 (s, B*F*$_4$).

Triphenyltelluronium chloride (3P-Te-Cl)

To synthesize 3P-Te-Cl, a Lewis acid-catalyzed reaction of the tellurium educt with benzene similar to Gunther *et al.*[43] was carried out (Fig. 2(b)). At first, 1 eq. (1.348 g, 5 mmol) of tellurium tetrachloride and 3 eq. (2.037 g, 15 mmol) of aluminium chloride were weighed into a 50 mL two-necked flask in a glove box to avoid hydrolysis of the precursor. The flask was equipped with a septum, a reflux condenser and a gas outlet at the top leading to gas washing bottles filled with sodium hydroxide solution. Argon atmosphere was maintained over the whole course of the reaction. Afterwards the educts were dissolved in 15 mL of dry benzene and the resulting yellow dispersion stirred magnetically. While the mixture was heated to 95 °C, there were several noticeable events. At around 70 °C, HCl formation started and the gas was forced up the condenser, through the gas washing bottles. This was achieved by constantly applying a slight stream of argon (balloon equipped with a needle outlet) through the septum of

the flask. When reaching around 80 °C, the mixture turned gray. As soon as the benzene started to reflux, the mixture was allowed to react for the next 70 min. The reaction was quenched by carefully pouring the mixture into 20 mL of iced water. A black precipitate formed immediately and leftover aluminium chloride was hydrolyzed. After filtering the dispersion via a glass frit, the dark precipitate (*ca* 3.1 g) was collected and dissolved in 13 mL of boiling distilled water. The solution was hot-filtered and allowed to cool to room temperature and afterwards stored at 2 °C to form colorless needle crystals (*ca* 1.4 g). Recrystallization from 3 mL of a 6:4 mixture of ethanol and chloroform led to colorless crystals which were washed with 10 mL of hexanes twice, followed by drying in vacuum. An amount of 1.184 g (60% of theory) of 3P-Te-Cl was obtained.

Melting point: 257.6–260.7 °C (lit. 249–250 °C)[43]; ^{1}H NMR (600 MHz, $CDCl_3$): 7.81 (d, 6H, 6× C–C*H*), 7.48 (t, 3H, 8× C–CH–CH–C*H*), 7.41 (t, 6H, C–CH–C*H*), 7.26 (s, $CDCl_3$); ^{13}C NMR (150 MHz, $CDCl_3$): 135.2 (s, 6× C–*C*H), 131.5 (s, 3× C–CH–CH–*C*H), 130.4 (s, 6× C–CH–*C*H), 128.8 (s, 3× Te–*C*), 77.2 (t, $CDCl_3$).

Triphenyltelluronium tetrafluoroborate (3P-Te-BF_4)

3P-Te-Cl was used in a procedure similar to that of Li *et al*.,[31] for an ion exchange reaction (Fig. 2(b)). To prepare 3P-Te-BF_4, at first 1 eq. (0.788 g, 2 mmol) of 3P-Te-Cl was dissolved in 6 mL of deionized water by gently applying heat to result in a clear solution. In the meantime, 1.05 eq. (0.231 g, 2.1 mmol) of sodium tetrafluoroborate was dissolved in 2 mL of deionized water. A clear solution was obtained after heating the mixture gently. After both solutions were allowed to cool to room temperature, their transparency was checked before moving on to the next step. The clear sodium tetrafluoroborate solution was added dropwise into the clear triphenyltelluronium chloride solution. A white precipitate started to form immediately and after 15 min of reaction time the reaction mixture was filtered via a glass frit. The solid was washed with 5 mL of deionized water twice to remove excess sodium tetrafluoroborate. After drying in vacuum, 3P-Te-BF_4 yielded 0.633 g (71% of theory) as a white powder.

Melting point: 211.5–215.2 °C (lit. 245–246 °C)[44]; ^{1}H NMR (600 MHz, $CDCl_3$): 7.64 (d, 6H, 6× C–C*H*), 7.61 (t, 3H, 3× C–CH–CH–C*H*), 7.53 (t, 6H, C–CH–C*H*), 7.26 (s, $CDCl_3$); ^{13}C NMR (150 MHz, $CDCl_3$): 134.9 (s, 6× C–*C*H), 132.9 (s, 3× C–CH–CH–*C*H), 131.3 (s, 6× C–CH–*C*H), 123.5 (s, 4× Te—*C*), 77.2 (t, $CDCl_3$); ^{19}F NMR (564 MHz, $CDCl_3$): −146.21 (s, B*F*$_4$), −146.26 (s, B*F*$_4$).

Verifying the absence of halogens

Approximately 10 mg of onium compound was dissolved in 0.5 mL of a 1:1 (v/v) mixture of methanol and deionized water or DMSO with a small amount of water, so the onium compound could stay in solution. After completely dissolving the substance (sometimes requiring additional heating), 0.5 mL of a saturated silver nitrate solution in the solvents mentioned above was added. The samples were mixed well and allowed to stand for 5 min and a white precipitated or cloudy solution (AgCl) indicated a positive test result.

Absorption characteristics

At first the onium salts were weighed into a small penicillin flask and dissolved in dry acetonitrile, achieving an aimed concentration of 1×10^{-3} mol L^{-1}. Afterwards the concentration was reduced to 1×10^{-4} and 1×10^{-5} mol L^{-1} by dilution of the samples by a factor of 10 and then again by a factor of 10. Then 3 mL of solution was transferred in 10 mm quartz cells for UV–visible spectroscopic experiments. Using a Lambda 750 UV–visible photometer, wavelengths from 250 to 600 nm, at a slit width of 2 nm, were measured.

Reduction potentials of onium salts

The onium compounds were weighed into brown-glass penicillin flasks and dissolved in 5 mL of a 0.5 mol L^{-1} solution of tetraethylammonium tetrafluoroborate in dry acetonitrile as an electrolyte. The sample solution was bubbled with argon gas for 3 min and all experiments were performed under light protection. A concentration of 0.01 mol L^{-1} of the tested initiators was used. Then 5 mL of the mixture was transferred into an IKA ElectraSyn 2.0 device containing a silver reference electrode which was filled with a 3 mol L^{-1} aqueous solution of KCl, a platinum working electrode and a platinum counter electrode. The scan was performed from 0 to +1.8 V, from there to −1.8 V and finally back to 0 V at a rate of 50 μV s^{-1}.

In advance of every new measurement and between every measurement, the electrodes, as well as the measurement chamber, were cleaned with acetone, followed by 1 N hydrochloric acid and finally rinsed with dry acetonitrile to ensure reproducibility.

Preparation of formulations based on BADGE/PC

The onium compounds were used in 1.16 mol% based on epoxy groups referred to BADGE and weighed into a small brown-glass vial. A master mix was prepared containing epoxy resin (78 wt%) and PC (22 wt%). An equal amount of master mix was added to the initiators. From here on two different substances were added to the formulations: 1.16 mol% of TPED for the subsequent simultaneous thermal analysis (STA) experiments and 1.16 mol % of anthracene for the Photo-DSC measurements. Afterwards the mixtures were homogenized using a vortex device, followed by 30 min of ultrasonic bath treatment at around 40 °C. If a compound did not dissolve well, the vial was gently heated with a heat gun up to around 50 °C for a short amount of time, followed by another treatment in the ultrasonic bath to improve solubility.

Thermal behavior of onium salts (RICP)

The formulations with 1.16 mol% onium salt and an equimolar amount of TPED, described in the formulations section, were used for all STA measurements using a Netsch 449 F1 JUPITER equipped with an autosampler. The temperature program started from 25 °C heating up to 350 °C at a rate of 10 K min^{-1}. Afterwards, the samples were cooled to 25 °C at a rate of 20 K min^{-1}. The prepared formulations were weighed in 13 ± 3 mg portions into small aluminium crucibles, which were closed by a pierced lid. Each crucible then was transported via the autosampler into the measuring chamber, which was flushed with nitrogen (40 mL min^{-1}) to maintain an inert atmosphere. The polymerization was induced by applying a temperature gradient. The exothermic behavior of the polymerization was recorded over time. Two determinations were made per formulation. The temperature at which the highest exothermic occurs is called T_{max}. Additionally, the temperature at which the polymerization started called T_{onset} was evaluated. Peak height correlates directly with the DSC (mW mg^{-1}) and the rate of polymerization R_P, higher values corresponding to higher reactivity of the measured system. For every sample, a duplet was measured. The epoxy group conversions were determined via Eqn (1)[45] and R_P was calculated via Eqn (2).[46] The theoretical heat of polymerization and the monomer density were taken from Table 2.

Table 2. Theoretical heat of polymerization ($H_{P,0}$) and density (ρ) of BADGE

Monomer	$H_{P,0}$ (kJ mol^{-1})	$H_{P,0}$ (J g^{-1})	ρ (g L^{-1})
BADGE[19]	194	570	1160

$$\mathrm{EGC}\,(\%) = \frac{\Delta H_P}{\Delta H_{P,0}} \times 100 \quad (1)$$

where ΔH_P is the heat of polymerization of the sample (J g^{-1}) and $\Delta H_{P,0}$ is the theoretical heat of polymerization (J g^{-1}).

$$R_P\,(\mathrm{mmol\,L^{-1}\,s^{-1}}) = \frac{\mathrm{DSC} \times \rho}{H_{P,0} \times 1000} \quad (2)$$

where DSC corresponds to the heat produced per mass unit of sample (mW mg^{-1}), ρ is the density of the monomer (g L^{-1}) and $\Delta H_{P,0}$ is the theoretical heat of polymerization (J g^{-1}).

Photoreactivity of onium salts

The prepared formulations were weighed in 12 ± 2 mg portions into small aluminium crucibles with a pipette. Each crucible then was transported via an autosampler into the measuring chamber of a Netsch 204 F1 Phoenix Photo-DSC, which was flushed with nitrogen to maintain an inert atmosphere. There was also a second crucible, the empty reference. The polymerization was induced by UV light of an OMNICURE 3000 Series with a wavelength of 320 to 500 nm (for sensitization experiments) or no wavelength filter at all (for the deep-UV study) and an intensity of 136 mW cm^{-2} at the sample. The exotherm of the polymerization was recorded over time. The polymerization was carried out isothermally at 25 °C. The samples were exposed for 300 s. Three determinations were made per formulation.

The time to the highest exotherm is called t_{max} (s). In the time-resolved DSC plot, this corresponds to that point in time at which the peak height *h* achieved its maximum. This value then subtracted for 5 s as this time corresponds to the internal delay of the measuring device. Peak height *h* correlates directly with the DSC (mW mg^{-1}) and the rate of polymerization R_P (mmol L^{-1} s^{-1}), higher values corresponding in higher reactivity of the measured system. The conversions were determined via Eqn (1) and R_P was calculated via Eqn (2). The theoretical heats of polymerization and the monomer densities were taken from Table 2.

RESULTS AND DISCUSSION

Selection and synthesis of tetrafluoroborate onium salts

When it comes to new cations as photoacid generators, there are several options on which to focus. Besides the diaryliodonium and triarylsulfonium salts commercially used in industry, phosphonium, selenonium, oxonium, telluronium, stibonium and many more are highly interesting for investigating as new (photo)acid generators.[47] The aim was the preparation of similar substituted onium compounds, containing different central atoms. Despite possible solubility issues of non-substituted phenyl rings in onium salts, the phenyl-only molecules were targeted. Simplicity was preferred over good solubility in nonpolar monomers. In addition, the solubility issues can be overcome by using formulations containing PC as a polarity-increasing component for the rather polar onium salts.[48] However, PC does not participate in cationic polymerization.[49]

Tetrafluoroborate was chosen to function as counterion in all synthesized species, due to the broad commercial availability and easy synthetic access of this specific anion, being aware of possible drawbacks such as the possibility of release of HF.[50] However, using counterions with significantly lower nucleophilicity such as hexafluorophosphates (PF_6), hexafluoroantimonates (SbF_6) or fluorinated borates will result in higher initiation efficiency and reactivity compared to BF_4.[2] The introduction of the tetrafluoroborate during every synthesis was aimed at guaranteeing a fair comparison in the tests afterwards. This limitation to tetrafluoroborates only is crucial to exclude effects of different anions and only cations are benchmarked to each other in later experiments.

Synthesis of the nine targeted onium salts was successfully carried out (Fig. 2). Complexity of the synthetic route and final yields vary significantly throughout the various salts. One outstanding example for poor yields is the triphenyloxonium salt, since an overall yield of around 0.15% was achieved. However, most reaction routes such as those for telluronium-, stibonium-, phosphonium- and bismuthonium-based onium salts show very good overall yields. For better comparison in the following reactivity studies, diphenyliodonium hexafluoroantimonate (2P-I-SbF_6) was synthesized using standard metathesis reaction starting from diphenyliodonium chloride and sodium hexafluoroantimonate.[31]

During the selection of possible onium salts for cationic polymerization, methylium and alkylated oxonium tetrafluoroborates were also tested. Triphenylmethylium tetrafluoroborate and alkoxylated tris(4-methoxyphenyl)methylium tetrafluoroborate were synthesized.[51] However, they hydrolyze during the mixing process with commercially available epoxy monomers and the resins harden in a few seconds. Premature hardening of the formulations during homogenization of the formulations was also a major issue with alkylated oxonium salts, such as trimethyl- and triethyloxonium tetrafluoroborate due to hydrolysis of the initiators. Despite those issues with carbon- and alkylated oxygen-based onium salts, a broad collection of onium salts can be tested in terms of photochemical behavior, redox potential and reactivity.

Absorption characteristics

During the photochemical analysis, the UV and visible light absorption spectra of the onium compounds were recorded. The wavelength range to scan started at 260 nm and went up to 500 nm. To determine which light source and wavelength filter were suitable in further experiments, samples were dissolved in dry acetonitrile. Depending on the absorption value of the onium salt, concentrations of 1×10^{-4} or 1×10^{-5} mol L^{-1} were used to ensure a linear correlation between concentration and absorption (Lambert–Beer law).

As illustrated in the absorption spectra (Fig. 3(a)), the commercially used 3P-S-BF_4 shows two maxima at 276 and 268 nm with a tail-out region to around 320 nm. 2P-I-BF_4 shows absorption starting at around 320 nm. The thiopyrylium-based 3PT-S-BF_4 shows broad absorption behavior with its peak at 361 nm ranging up to 460 nm. The pyridinium-based salt 2BuMeP-N-BF_4 shows a small peak at 263 nm, while the regions above 280 nm show no absorption at all. Considering the phosphonium-based onium salt 4P-P-BF_4, one can clearly notice two peaks at approximately 270 nm, which is in accordance with the literature.[19] The data

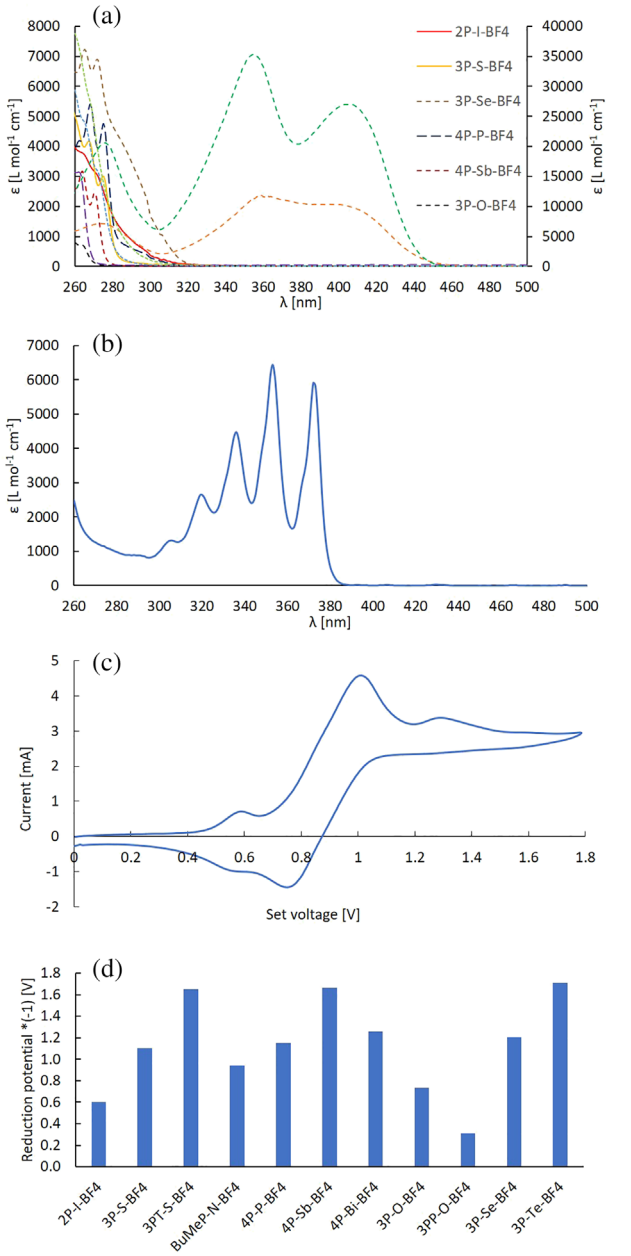

Figure 3. (a) Wavelength dependence of molar extinction coefficient for onium salts (1×10^{-4} or 1×10^{-5} mol L^{-1}) in acetonitrile (3PT-S-BF_4 and 3PP-O-BF_4 are displayed on the secondary *y*-axis). (b) Wavelength dependence of molar extinction coefficient for anthracene. (c) Voltammogram of ferrocene (0.01 mol L^{-1}) measured in dry acetonitrile buffer (0.5 mol L^{-1} tetraethylammonium tetrafluoroborate); CV: 0 V → +1.8 V → −1.8 V → 0 V at 50 μV s^{-1}. (d) Reduction potential ($E_{p,c}$) of onium salts (0.01 mol L^{-1}) measured in dry acetonitrile buffer (0.5 mol L^{-1} tetraethylammonium tetrafluoroborate); CV: 0 V → +1.8 V → −1.8 V → 0 V at 50 μV s^{-1}.

obtained for solutions containing 4P-Sb-BF_4 show two absorption maxima in the measured range (271 and 264 nm) with extinction coefficients above 2400 L mol^{-1} cm^{-1}. The bismuth-based onium salt 4P-Bi-BF_4 shows no absorption peak in the measured range; however, at lower wavelengths, starting at around 310 nm, a strong absorption is obtained. As expected, 3PP-O-BF_4 with its four aromatic rings reaches the highest value in terms of molar extinction coefficient, as well as two maxima at 357 and 409 nm. The absorption maximum for the oxonium salt 3P-O-BF_4 in the measured range is visible at 264 nm with an extinction coefficient of around 700 L mol^{-1} cm^{-1}. The selenium-based compound 3P-Se-BF_4 shows its maxima at 319 and 267 nm, while the tellurium-based onium salt 3P-Te-BF_4 shows no peak in the scanned region; however, strong absorption starts below 290 nm.

Anthracene has four distinct maxima ranging from 320 to 372 nm, making it a versatile sensitizer for UV-based applications (Fig. 3(b)).[1]

Reduction potentials of onium salts

To investigate the reduction and oxidation potentials, cyclic voltammetry (CV) was used. By sweeping the applied potential on a sample, a change in current flow is detected. Therefore, CV can determine at which potentials reactions or changes of the sample occur. In the case of CV, two potentials are chosen and the applied current cycles back and forth between those values. The values for the two aimed potentials have to be considered carefully, due to dependence of the sample used and the critical potential for the solvent, at which it starts to decompose. If the reactions or processes are reversible, this measurement method is repeatable. Peak potentials in the voltammogram can be reduction potentials $E_{p,c}$ or oxidation potentials $E_{p,a}$ and together they can form the half-wave potential of a redox couple represented in Eqn (3). A reversible voltammogram is independent of the applied scan rate, due to a normalizing procedure. The values for the peak potentials $E_{p,c}$ and $E_{p,a}$ stay the same by dividing by the square root of the scan rate.

$$E_{1/2} = \frac{E_{p,c} + E_{p,a}}{2} \tag{3}$$

where $E_{p,c}$ is the maximum reduction potential (V) and $E_{p,a}$ is the maximum oxidation potential (V).

If a reaction is nonreversible, the obtained voltammogram contains only one peak, which is either an oxidation or reduction potential. This can be observed if a compound is decomposing due to the applied voltage, which is the case for onium salts. Another characteristic of irreversible reactions is the dependence of the peak potentials on the scan rate. Therefore, it should be the same for all experiments. CV measurements only provide an estimated value for an electron transfer on a platinum surface. It is very important to measure samples like onium compounds under the same experimental conditions. The sample solutions were bubbled with argon gas to replace the oxygen in solution and all measurements were conducted under light protection. The obtained reduction peak voltages are normalized by referring them to the half-wave potential of ferrocene. Due to this normalization step all obtained values are comparable to each other. Also, the measurement data are unaffected by using new electrodes (as long as they are of the same material and show the same surface area) or a different bottle of solvent. The literature value for ferrocene in acetonitrile at a scan rate of 50 μV s^{-1} and room temperature (298.15 K) is $E_{1/2}$ = 0.992 V.[52]

CV was performed with all onium-based samples to investigate their reduction potential for further studies involving sensitization or radical-induced decomposition. This experiment involved a buffer of tetraethylammonium tetrafluoroborate in dry acetonitrile as an electrolyte for all samples. Additionally, ferrocene was measured for a normalizing step. Thus, the sample potentials were referred to the ferrocene half-wave potential. This step ensures a valid comparison across all onium salts measured.

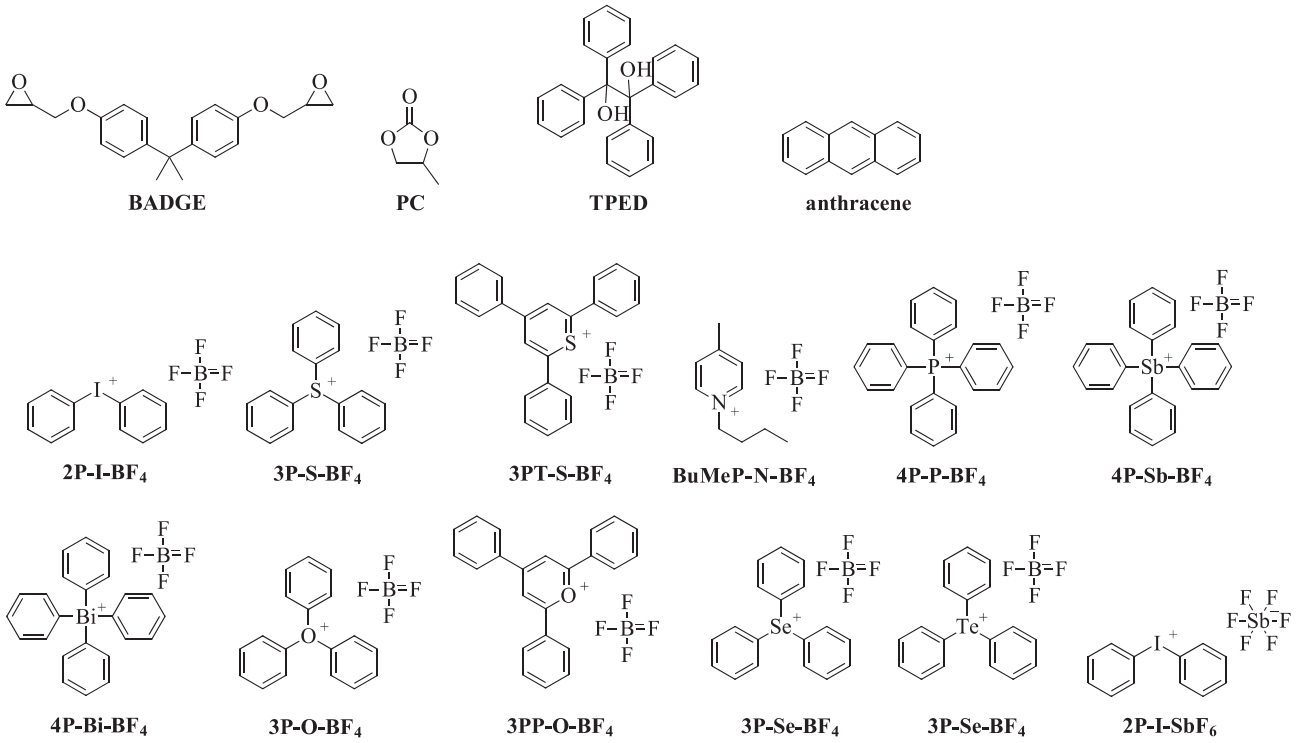

Figure 4. Monomer BADGE, additives PC, TPED and anthracene and the different onium salts as initiators.

The oxidation of ferrocene occurs at 1.00 V, while the reduction peak is at 0.76 V, resulting in a half-wave potential of $E_{1/2} = 0.88$ V (Fig. 3(c)). Therefore, the measurement method is normalized for all future measurements due to the comparison to ferrocene as a standard to all sample potentials.

The resulting reduction potentials give basic information of how hard it is for an electron to be up taken by the tested molecule (Fig. 3(d)). A higher reduction potential leads to an increased effort to make this electron uptake happen. The lowest reduction potential is achieved for 3PP-O-BF_4 at around 0.3 V. The iodonium salt 2P-I-BF_4 shows a potential of 0.65 V, followed by 3P-O-BF_4 at around 0.7 V. The nitrogen-based pyridinium salt 2BuMeP-N-BF_4 reaches a reduction potential of 0.9 V, while the sulfonium compound 3P-S-BF_4 exhibits a reduction potential of 1.1 V. That of the phenylated phosphonium compound is in the region of 1.2 V, together with the selenium-based molecule. 4P-Bi-BF_4 shows a reduction potential of around 1.3 V. The highest voltage values are obtained by measuring 3P-Te-BF_4, 4P-Sb-BF_4 and 3PT-S-BF_4 with reduction potentials of 1.6 to 1.7 V.

Formulations based on BADGE/PC

For reactivity studies, formulations based on a cationically polymerizable monomer had to be prepared. This mixture's main component was the epoxy monomer BADGE. To ensure good solubility of the rather polar onium salts in the nonpolar monomer environment, PC was used as a polarity-adjusting agent (Fig. 4). However, PC does not participate in cationic polymerization.[49]

The onium salts were used in 1.16 mol% based on epoxy groups referred to BADGE. The final formulations contain 78 wt% epoxy resin and 22 wt% PC. For the STA study, an equimolar amount of TPED compared to the onium salt was added, and for the sensitization experiments with the Photo-DSC, an equimolar amount of anthracene compared to the onium salt was added.

To present the reactivity difference of tetrafluoroborates and the significantly lower nucleophilic hexafluoroantimonates, all studies were additionally performed with 2P-I-SbF_6.

Thermal behavior of onium salts

During the STA experiments, the suitability of onium salts for RICP was investigated. Onium compounds are known to decompose by thermally generated radicals from C–C labile compounds.[48] TPED is known to start decomposition and thermal radical formation above 40 °C.[53,54] The thermal radicals are able to attack the acid generator, which is liberating the superacid, and finally initiate polymerization of the resin under nitrogen. This investigation was necessary to know exactly above which onset temperature polymerization can occur in combination with TPED. All STA experiments with TPED as C–C labile compound were conducted from 25 to 250 °C at a heating rate of 10 K min^{-1}.

State-of-the-art iodonium salt shows an onset temperature of 140 °C and a T_{max} value of 150 °C (Fig. 5(a)). The triphenyloxonium-based acid generator shows the highest temperature at the highest exothermic and onset temperature, both above 214 °C. On the lower end, the pyrylium salt 3PP-O-BF_4 shows an onset temperature of 129 °C.

Considering the rate of polymerization (Fig. 5(b)), one can clearly notice the advantageous behavior of the iodonium-based salt with a value of around 46 mmol L^{-1} s^{-1}. The closest values to this benchmark are those of 4P-Bi-BF_4 as well as 3PP-O-BF_4 at 18 and 17 mmol L^{-1} s^{-1}. Conversions reach up to 98% for the iodonium-based 2P-I-BF_4. With 85% conversion, 4P-Bi-BF_4 performs quite well in BADGE. The pyrylium salt 3PP-O-BF_4 reaches around 75% conversion. The lower nucleophilic iodonium hexafluoroantimonate 2P-I-SbF_6 outperformed the tetrafluoroborate in all metrics as expected. The results showed a 10 to 15 °C lower

Polymer International published by John Wiley & Sons Ltd on behalf of Society of Industrial Chemistry.

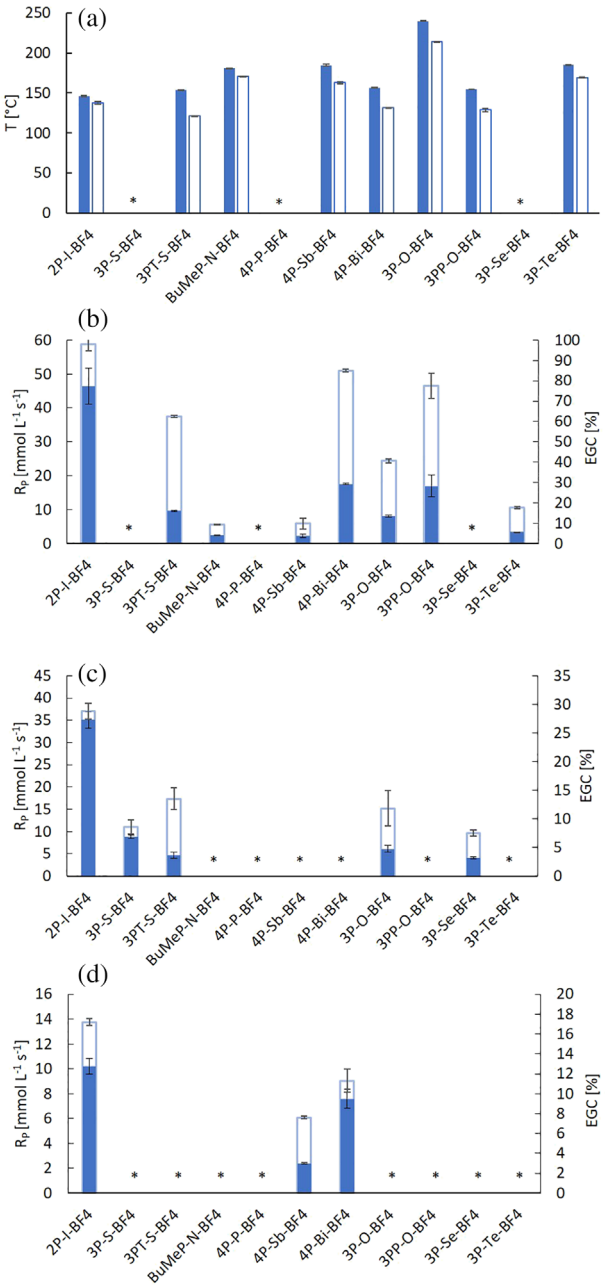

Figure 5. (a) Temperature at the highest exothermic (T_{max}; filled columns) and polymerization onset temperature (T_{onset}; open columns) in BADGE/PC with TPED and onium tetrafluoroborates. *Missing columns represent insufficient exothermicity detected during the STA. (b) Rate of polymerization (filled columns) and epoxy group conversion (open columns) in BADGE/PC with TPED and onium tetrafluoroborates. (c) Rate of polymerization (filled columns) and epoxy group conversion (open columns) in the deep-UV study in BADGE/PC of onium tetrafluoroborates. (d) Rate of polymerization (filled columns) and epoxy group conversion (open columns) sensitized by anthracene in BADGE/PC of onium tetrafluoroborates.

onset and maximum temperature, as well as a 230% increase in R_P while retaining the same conversions as 2P-I-BF_4.

Photoreactivity of onium salts

Deep-UV study

The main objective of the deep-UV study was to investigate the potentials of all onium salts as photoacid generators. Since the UV–visible experiments indicated a broad range of absorption across the tested onium compounds, a broadband mercury lamp was used as irradiation source. The emission spectrum ranges from around 250 to 650 nm. Across the subsequent deep-UV experiments, no sensitizer was used in the formulations, only the onium salt in the BADGE/PC mixture.

The iodonium salt does outstandingly well (Fig. 5(c)) with a value of 35 mmol L^{-1} s^{-1}. However, most onium salts do not show any exothermic behavior. Interestingly, the bismuth-based 4P-Bi-BF_4 and the tellurium-based 3P-Te-BF_4 do show a very strong endothermic behavior during the polymerization, which could not be explained trivially. The samples were totally cured after irradiation. However, no exothermic peak could be obtained in several measurements. The reason behind this observation may be the evaporation of the PC polarity-adjusting agent. However, no significant decrease in mass of the crucible plus the sample after the measurement could be determined. The conversion of the iodonium-based salt reaches around 29%. All other onium salts afforded conversions below 14%.

In addition, the reactivity of 2P-I-SbF_6 and 2P-I-BF_4 was compared. As expected, during the deep-UV study, an increase of 220% in rate of polymerization can be observed, while maintaining the same conversions.

Sensitization of onium salts

To investigate the efficiency of the potential sensitizers, a Photo-DSC study was performed with the onium salts and anthracene as sensitizing compound. Starting with the sensitization of the onium compounds, the series of measurements should give basic information about the reactivity. The more reactive an initiator–sensitizer system, the better is the overall initiation efficiency and curing of the material. Anthracene shows its absorption maxima from 320 to 370 nm, with a tail-out region reaching up to 380 nm. Therefore, a UV source with a 320–500 nm filter was used in this series of experiments.

Comparing the reactivity of the onium salts, one can clearly see the advantage of using the commercially established iodonium compound 2P-I-BF_4, achieving 10 mmol L^{-1} s^{-1} (Fig. 5(d)). The second highest rate is obtained in a formulation containing the bismuth-based 4P-Bi-BF_4 at 8 mmol L^{-1} s^{-1}. The only other onium compound to achieve an exothermic behavior at all, besides the iodine- and bismuth-based ones, is the chemically very similar (same group in periodic table of elements) 4P-Sb-BF_4 with a rather low rate of polymerization of around 2 mmol L^{-1} s^{-1}. Considering the overall epoxy conversion, one can clearly see the benefit of iodonium salts at around 17% conversion, compared to the 11% for 4P-Bi-BF_4 and 8% for the antimony-based salt.

Additionally, 2P-I-SbF_6 was benchmarked against its tetrafluoroborate counterpart 2P-I-BF_4. The results showed a 236% increase in R_P while maintaining the same conversion as the BF_4 salt.

CONCLUSIONS

With the introduction of onium salt, a highly efficient approach for the photopolymerization of cationic monomers was made. Multiple initiation pathways are possible to liberate the superacid from the onium salt, subsequently initiating the polymerization reaction. The decomposition reaction can be triggered on demand by absorption of a photon, input of thermal energy, generated radicals or the use of sensitizers. This versatility makes state-of-the-art iodonium and sulfonium salts a popular choice as cationic initiators. The challenge to produce a new, highly efficient photoacid generator like iodonium and sulfonium salts is quite difficult, since a lot of basic research on this topic has already been performed.

After a screening of many group 14 to 16 elements, which could be transformed into their onium species rather easily, a few promising candidates could be obtained. The main issue during the investigation of the tetrafluoroborates was the solubility in non-polar media like most commercial epoxides. Therefore, a quite high amount of PC has to be used to completely dissolve the onium salts. Mainly bismuthonium and pyrylium salts showed promising results during the reactivity tests and were compared to the state-of-the-art iodonium and sulfonium salts. The reactivity of 4P-Bi-BF_4 reached up to 74% compared to 2P-I-BF_4 in the epoxy-based monomer BADGE with the thermal radical initiator TPED and quite good reactivity in formulations containing the sensitizer anthracene (64% of the reactivity of the iodonium salt). More detailed information regarding bismuth- and pyrylium-based salts in cationic polymerization can be obtained from a previously published paper.[55] However, the deep-UV study shows thiopyrylium, oxonium and selenonium salts are of photochemical interest as well. Additionally, bismuthonium and stibonium salts show great potential towards sensitization with anthracene.

ACKNOWLEDGEMENT

The authors acknowledge TU Wien Bibliothek for financial support through its Open Access Funding Program.

CONFLICT OF INTEREST

The authors declare no conflict of interest. The data that support the findings of this study are available on request from the corresponding author. The data are not publicly available due to privacy or ethical restrictions.

REFERENCES

1 Crivello JV, Dietliker K and Bradley G, *Photoinitiators for Free Radical Cationic & Anionic Photopolymerisation*. Wiley, Hoboken, NJ, pp. 329–373 (1999).
2 Green WA, *Industrial Photoinitiators: A Technical Guide*. Taylor & Francis, Boca Raton, FL, Chap. 7 (2010).
3 Fouassier J-P, *Photoinitiation, Photopolymerization, and Photocuring: Fundamentals and Applications*. Hanser, Munich, pp. 95–106 (1995).
4 Crivello JV and Lam JHW, *Macromolecules* **10**:1307–1315 (1977).
5 Crivello JV, *J Polym Sci Polym Chem* **37**:4241–4254 (1999).
6 Crivello JV and Lam JHW, *J Polym Sci Polym Chem* **17**:977–999 (1979).
7 Dadashi-Silab S, Doran S and Yagci Y, *Chem Rev* **116**:10212–10275 (2016).
8 Bulut U and Crivello JV, *Macromolecules* **38**:3584–3595 (2005).
9 Abdulrasoul FAM, Ledwith A and Yagci Y, *Polym Bull* **1**:1–6 (1978).
10 Cook WD, Chen SH, Chen F, Kahveci M and Yagci Y, *Abstr Pap Am Chem S* **238**:263–264 (2009).
11 El-Roz M, Lalevee J, Morlet-Savary F, Allonas X and Fouassier JP, *J Polym Sci Polym Chem* **46**:7369–7375 (2008).
12 Meerwein H and van Emster K, *Ber Dtsch Chem Ges* **55**:2500–2528 (1922).
13 Kraus CA and Foster LS, *J Am Chem Soc* **49**:457–467 (1927).
14 Olah GA, Laali KK, Wang Q and Prakash GKS, *Onium Ions*. Wiley, Hoboken, NJ, pp. 391–424 (1998).
15 Edlund U, Arshadi M and Johnels D, *J Organomet Chem* **456**:57–60 (1993).
16 Boyer NE, Methoden der organischen chemie (houben–weyl) vol. xii, part I, in *Organische Phosphorverbindungen*, ed. by Sasse K and Muller E. Georg Thieme Verlag, Stuttgart (1963).
17 Schmidbaur H, *Inorg Synth* **18**:135–140 (1978).
18 Takuma K, Takata T and Endo T, *Macromolecules* **26**:862–863 (1993).
19 Atmaca L, Kayihan I and Yagci Y, *Polymer* **41**:6035–6041 (2000).
20 Pan B and Gabbaï FP, *J Am Chem Soc* **136**:9564–9567 (2014).
21 Matano Y, Shinokura T, Yoshikawa O and Imahori H, *Org Lett* **10**:2167–2170 (2008).
22 Meerwein H, Hinz G, Hofmann P, Kroning E and Pfeil E, *I J Praktische Chemie* **147**:257–285 (1937).
23 Nesmeianov AN and Tolstaia TP, *Dokl Akad Nauk SSSR* **117**:626–628 (1957).
24 Nesmeyanov AN and Tolstaya TP, *Bull Acad Sci USSR, Div Chem Sci* **8**: 620–623 (1959).
25 Umemoto T, Adachi K and Ishihara S, *J Org Chem* **72**:6905–6917 (2007).
26 Lecompère M, Allonas X, Maréchal D and Criqui A, *Macromol Rapid Commun* **38**:1600660 (2017).
27 Irgolik KJ, Organotellurium compounds, in *Methods of Organic Chemistry*, 4th edn, ed. by Klamann D. G. Thieme Verlag, Stuttgart (1990).
28 Crivello JV and Lam JHW, *J Polym Sci Polym Chem* **17**:1047–1057 (1979).
29 Korwar S, Burkholder M, Gilliland SE, Brinkley K, Gupton BF and Ellis KC, *Chem Commun* **53**:7022–7025 (2017).
30 Kraszkiewicz L and Skulski L, *Synthesis-Stuttgart* **15**:2373–2380 (2008).
31 Li, Y.; Yantian, H.; Zaosheng, L., One alkyl triphenyl substituted group based phosphonium salt preparation method and application. 2017, Patent CN107129511.
32 Makarova LG and Nesmeianov AN, *Dokl Akad Nauk SSSR* **50**:617–626 (1945).
33 Michaudel Q, Chauvire T, Kottisch V, Supej MJ, Stawiasz KJ, Shen LX *et al*., *J Am Chem Soc* **139**:15530–15538 (2017).
34 Kharchenko VG, Chalaya SN, Noritsina MV and Kulikova LK, *Khimiko-Farmatsevticheskii Zhurnal* **10**:80–83 (1976).
35 Ma YQ, Li JS, Xuan ZN and Liu RC, *J Organomet Chem* **620**:235–242 (2001).
36 Solyntjes S, Neumann B, Stammler HG, Ignat'ev N and Hoge B, *Chem Eur J* **23**:1568–1575 (2017).
37 Moiseev DV, Malysheva YB, Shavyrin AS, Kurskii YA and Gushchin AV, *J Organomet Chem* **690**:3652–3663 (2005).
38 Challenger F and Wilkinson JF, *J Chem Soc* **121**:91–104 (1922).
39 Matano Y, Azuma N and Suzuki H, *J Chem Soc Perkin Trans 1* **13**:1739–1747 (1994).
40 Matano Y, Begum SA, Miyamatsu T and Suzuki H, *Organometallics* **17**: 4332–4334 (1998).
41 Flood DT, *Org Synth* **13**:46–50 (1933).
42 Wittig G and Fritz H, *Ann Chem Justus Liebig* **577**:39–46 (1952).
43 Gunther WHH, Nepywoda J and Chu JYC, *J Organomet Chem* **74**:79–84 (1974).
44 Rainville DP and Zingaro RA, *J Organomet Chem* **190**:277–288 (1980).
45 Menczel JD and Prime RB, *Thermal Analysis of Polymers: Fundamentals and Applications*. Wiley, Hoboken, NJ, Chap. 2 (2014).
46 Flory PJ, *Principles of Polymer Chemistry*. Cornell University Press, Munich, Chap. 11 (1953).
47 Tsuchimura T, *J Photopolym Sci Technol* **33**:15–26 (2020).
48 Bomze D, Knaack P and Liska R, *Polym Chem-Uk* **6**:8161–8167 (2015).
49 Kricheldorf HR and Jenssen J, *J Macromol Sci Chem* **A26**:631–644 (1989).
50 Freire MG, Neves CMSS, Marrucho IM, Coutinho JAP and Fernandes AM, *J Phys Chem A* **114**:3744–3749 (2010).
51 Karim A, Schulz N, Andersson H, Nekoueishahraki B, Carlsson ACC, Sarabi D *et al*., *J Am Chem Soc* **140**:17571–17579 (2018).
52 Tsierkezos NG, *J Solution Chem* **36**:289–302 (2007).
53 Bledzki A and Braun D, *Makromol Chem* **182**:1047–1056 (1981).
54 Braun D and Becker KH, *Angew Makromol Chem* **6**:186 (1969).
55 Taschner R, Knaack P and Liska R, *J Polym Sci* **59**:1841–1854 (2021).

